Research Article | Vol. 24, No. 23 | 14 Nov 2016 | OPTICS EXPRESS 26055

Optics EXPRESS

Optical magnetization, Part II: Theory of induced optical magnetism

ALEXANDER A. FISHER,[1,2] ELIZABETH F. C. DREYER,[2] AYAN CHAKRABARTY,[2] AND STEPHEN C. RAND[1,2,*]

[1]*Division of Applied Physics, University of Michigan, Ann Arbor, MI 48109, USA*
[2]*Center for Dynamic Magneto-Optics, Dept. of Electrical Engineering & Computer Science, University of Michigan, Ann Arbor, MI 48109-2099, USA*
[*]*scr@umich.edu*

Abstract: A fully quantized analysis is presented on the origin of induced magnetic dipole (MD) scattering in two-level diatomic molecules. The interaction is driven by dual optical fields, E and H^*, and is universally allowed in dielectric optical materials, including centrosymmetric media. Leading terms of the interaction are shown to be quadratic and cubic with respect to the intensity, predicting an upper limit for the induced magnetic dipole scattering intensity ($I_{MD} \propto m^2$) that is equal to the electric dipole scattering ($I_{ED} \propto p^2$). The optical dynamics proceed by first establishing an electric polarization in the system. Then the magnetic field exerts torque on the orbital angular momentum of the excited state, mediating an exchange of orbital and rotational angular momenta that enhances the magnetic moment. The magneto-electric interaction also accounts for second-order, unpolarized scattering from high-frequency librations previously ascribed to third-order, all-electric processes.

OCIS codes: (190.0190) Nonlinear optics; (190.4410) Nonlinear optics, parametric processes; (190.7110) Ultrafast nonlinear optics; (320.7110) Ultrafast nonlinear optics; (350.3618) Left-handed materials.

References and links

1. J. C. Ginn, I. Brener, D. W. Peters, J. R. Wendt, J. O. Stevens, P. F. Hines, L. I. Basilio, L. K. Warne, J. F. Ihlefeld, P. G. Clem, and M. B. Sinclair, "Realizing optical magnetism from dielectric metamaterials," Phys. Rev. Lett. **108**(9), 097402 (2012).
2. W. F. Koehl, B. B. Buckley, F. J. Heremans, G. Calusine, and D. D. Awschalom, "Room temperature coherent control of defect spin qubits in silicon carbide," Nature **479**(7371), 84–87 (2011).
3. G. D. Fuchs, G. Burkard, P. V. Klimov, and D. D. Awschalom, "A quantum memory intrinsic to single nitrogen–vacancy centres in diamond," Nat. Phys. **7**(10), 789–793 (2011).
4. C. D. Stanciu, F. Hansteen, A. V. Kimel, A. Kirilyuk, A. Tsukamoto, A. Itoh, and T. Rasing, "All-optical magnetic recording with circularly polarized light," Phys. Rev. Lett. **99**(4), 047601 (2007).
5. W. M. Fisher and S. C. Rand, "Optically-induced charge separation and terahertz emission in unbiased dielectrics," J. Appl. Phys. **109**(6), 064903 (2011).
6. S. L. Oliveira and S. C. Rand, "Intense nonlinear magnetic dipole radiation at optical frequencies: molecular scattering in a dielectric liquid," Phys. Rev. Lett. **98**(9), 093901 (2007).
7. S. C. Rand, W. M. Fisher, and S. L. Oliveira, "Optically induced magnetization in homogeneous, undoped dielectric media," J. Opt. Soc. Am. B **25**(7), 1106 (2008).
8. W. M. Fisher and S. C. Rand, "Dependence of optically induced magnetism on molecular electronic structure," J. Lumin. **129**(12), 1407–1409 (2009).
9. K. Y. Bliokh, Y. S. Kivshar, and F. Nori, "Magnetoelectric effects in local light-matter interactions," Phys. Rev. Lett. **113**(3), 033601 (2014).
10. A. Einstein and W. J. de Haas, "Experimental proof of the existence of Ampère's molecular currents," K. Akad. van Wet. Amsterdam, Proc. **18**, 696–711 (1915).
11. A. A. Fisher, E. F. C. Dreyer, A. Chakrabarty, and S. C. Rand, "Optical magnetization, Part I: Experiments on radiant optical magnetization in solids," Opt. Express **24**(23), 26076–26091 (2016).
12. N. A. Spaldin and M. Fiebig, "Materials science. The renaissance of magnetoelectric multiferroics," Science **309**(5733), 391–392 (2005).
13. V. B. Berestetskii, E. M. Lifshitz, and L. P. Pitaevskii, *Quantum Electrodynamics*, 2nd ed. (Butterworth-Heinemann, 1982), Vol. 4.
14. A. A. Fisher, E. F. Cloos, W. M. Fisher, and S. C. Rand, "Dynamic symmetry-breaking in a simple quantum model of magneto-electric rectification, optical magnetization, and harmonic generation," Opt. Express **22**(3), 2910–2924 (2014).

#275606 http://dx.doi.org/10.1364/OE.24.026055
Journal © 2016 Received 9 Sep 2016; accepted 26 Oct 2016; published 1 Nov 2016

Optics EXPRESS

15. G. Herzberg, *Spectra of Diatomic Molecules*, 2nd ed. (Van Nostrand Reinhold, 1950).
16. C. Cohen-Tannoudji and S. Reynaud, "Dressed Atom Approach to Resonance Fluorescence," in *Multiphoton Processes*, J. Eberly and P. Lambropoulos, eds. (J. Wiley & Sons Inc., 1977), pp. 103–118.
17. S. C. Rand, *Lectures on Light*, 2nd ed. (Oxford University Press, 2016).
18. C. H. Townes and A. L. Schawlow, *Microwave Spectroscopy* (Dover, 1975).

1. Introduction

New methods of attaining high-frequency magnetism are of relevance to many fields, including metamaterials, spintronics, quantum information, and data storage. In recent years novel applications of electromagnetism have emerged from the search for negative permeability in structured materials [1], coherent optical spin control of semiconductor charge carriers [2] or luminescent centers [3], and ultrafast switching of magnetic domains [4]. As a consequence, any prospect of eliciting magnetic response from natural, unstructured, "non-magnetic" materials can be expected to accelerate the development of magneto-photonic technologies based on magnetic interactions. The realization of strong optical magnetism in nominally "non-magnetic" media for example could lead to novel forms of light-by-light switching, energy conversion, negative permeability in natural materials or the generation of large (oscillatory) magnetic fields without current-carrying coils [5–8]. In this paper, a magneto-electric optical process is shown to induce strong magnetization at the molecular level [9] through a mechanism that is somewhat reminiscent of the Einstein-de Haas effect [10]. However, in the present all-optical interaction, both "internal" and "external" motions of constituents of the medium are driven by light. This multi-photon process enhances magnetic response by first depositing orbital angular momentum in a molecule and then converting it with magneto-optic torque to molecular rotation in such a way that a magnetic moment as large as the electric dipole transition moment may be realized. Validation of this theory is provided by experimental observations in a companion paper [11].

Magneto-electric (M-E) phenomena have been investigated at the macroscopic level in solids for some time with technological objectives similar to those mentioned above. M-E materials invariably include a magnetic constituent and their applications vary from electric power generation via magnetostriction to the use of electric fields to control magnetic domains. However M-E effects tend to be relatively slow and weak, even in specially engineered materials (ferro-electrics, ferro-magnets, multi-ferroics and the like [12]). The limitations relate to the intermediate fields required to mediate an overall M-E response. In magnetic materials lacking inversion symmetry, as an example, the application of a magnetic field causes strain via magnetostriction and subsequently a voltage can be generated as the result of a strain-induced piezoelectric effect. In such situations the internal strain field is an intermediary in the M-E effect, causing the voltage to be an indirect, rather than a direct, result of applying the magnetic field.

In this article a magneto-electric mechanism is analyzed that is intense and fast because it operates directly at the molecular level to produce a radiant magnetization, $M = \chi EH^*$. The optical interaction is governed by combined parity-time (P-T) symmetry and can therefore take place in centrosymmetric media [9,13]. We focus on the dynamics of a simple, 2-level molecular model that produces magnetization by a second-order nonlinear optical process driven jointly by the electric and magnetic field components of light. In an earlier publication, it was found that no specialized symmetry or material property was necessary to support second-order magneto-electric interactions due to parity violation, but that in spinless atoms no mechanism existed to enhance induced effects such as magnetization [14]. In atoms, magnetic transitions invariably take place at frequencies much smaller than the optical frequency, so that resonance driven directly by optical fields is not possible and magnetic dipole effects are negligible. In stark contrast to this, it is shown here that very strong magnetic dipole effects can take place in molecular media because torque dynamics make optical magnetic resonance possible at elevated field strengths. While other nonlinear interactions in principle can make finite contributions, electric quadrupole and higher order

Optics EXPRESS

multipole contributions are ignored throughout this treatment on the basis that they are smaller than electric dipole moments by the square of the wavenumber times the particle radius, estimated to be $(ka)^2 < 10^{-5}$ at optical frequencies.

The present treatment quantizes both internal and external degrees of freedom of the molecule as well as the optical electric and magnetic fields, furnishing a closed form solution that is not possible in a spinless atomic model. Magnetic torque dynamics are shown to provide sufficient enhancement of magnetization to achieve equality between induced electric and magnetic moments in the high intensity limit. This result is confirmed experimentally in [11], hereafter referred to simply as I. The intensity required to reach maximum magnetization (relative to electric polarization) is shown to scale inversely with the rotation/libration frequency of the molecule.

2. Model for molecular ME-magnetization

The model considered here consists of a homonuclear diatomic molecule (symmetric top) with a 1-photon electric dipole (*ED*) resonance at frequency ω_0 [15]. The quantization axis is assumed to lie along $\hat{x}$, the axis of the molecule, and is parallel to the electric field. Linearly-polarized light of frequency ω with a small 1-photon detuning of $\Delta \equiv \omega_0 - \omega$ propagates along $\hat{z}$. The ground electronic state is taken to be $^1\Sigma_g^+$, the excited state $^1\Pi_u$, and orbital angular momentum is specified by the eigenvalue of L and its projection m_l (or Λ) on the axis. Uncoupled electronic states are denoted by $|\alpha L m_l\rangle$, with $\alpha = 1,2$ specifying the principal quantum number. The basis states support an *ED* transition from $L=0$ to $L=1$ followed by a magnetic dipole (*MD)* transition from $m_l = 0$ to $m_l = \pm 1$. The basis set comprises the four states $|100\rangle, |210\rangle, |21-1\rangle$ and $|211\rangle$. To simplify the presentation, basis state $|211\rangle$ will be omitted from much of the development. This has the benefit of reducing the dimensionality of the eigenvalue problem from 4×4 to 3×3, making an approximate analytic solution possible while introducing only a small error in the calculated magnetic moment. At the end of the paper, state $|211\rangle$ is reinserted into the basis set to provide numerically exact results that achieve quantitative agreement with experimental results in companion paper I.

In our pedagogical 3-state model, molecular rotational states are written $|Om_o\rangle$ and comprise only $|00\rangle$, $|10\rangle$ and $|11\rangle$ (see Appendix A). The optical field is assumed to be a single-mode Fock state $|n\rangle$. The molecule-field states therefore form the uncoupled product states $|1\rangle \equiv |100\rangle|00\rangle|n\rangle, |2\rangle \equiv |210\rangle|10\rangle|n-1\rangle$, and $|3\rangle \equiv |21-1\rangle|11\rangle|n\rangle$. These are eigenstates of the molecule-field Hamiltonian

$$\hat{H}_{mf} = \hat{H}_{mol} + \hat{H}_{field} = (\hbar\omega_0/2)\hat{\sigma}_z + \hat{O}^2/2I + \hbar\omega\hat{a}^+\hat{a}^-, \tag{2.1}$$

with eigenenergies $E_i (i = 1,2,3)$ defined by $\hat{H}_{mf}|i\rangle = E_i|i\rangle$. $\hat{O}^2/2I$ designates kinetic energy of molecular rotation perpendicular to the internuclear axis with moment of inertia *I*. Basis state energies are:

$$E_1 = -\frac{\hbar\omega_0}{2} + n\hbar\omega, \tag{2.2}$$

$$E_2 = E_1 + \hbar\Delta = \frac{\hbar\omega_0}{2} + (n-1)\hbar\omega, \tag{2.3}$$

Optics EXPRESS

$$E_3 = E_2 - \hbar\Delta + \hbar\omega_\phi = -\frac{\hbar\omega_0}{2} + n\hbar\omega + \hbar\omega_\phi. \tag{2.4}$$

In Eq. (2.1) above, $\hat{\sigma}_z$ is a Pauli spin operator. $\hat{a}^+$ and $\hat{a}^-$ are raising and lowering operators of the single mode field respectively. The sign of the first term on the right of Eq. (2.4) reflects the fact that state 3 has rotational energy $\hbar\omega_\varphi \equiv \hbar^2 / I$ but no internal electronic kinetic energy (i.e. no electronic excitation), consistent with a 2-photon interaction that terminates in a rotationally-excited ground state sublevel (as depicted in Fig. 1).

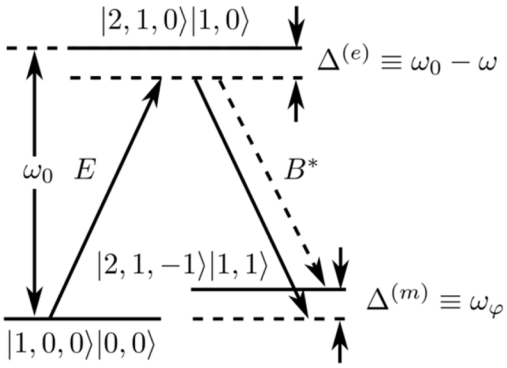

Fig. 1. Energy levels of the molecular model showing the 2-photon transition (solid arrows) driven by the optical E and B^* fields The dashed downward arrow depicts a magnetic de-excitation channel that becomes an option if the excitation bandwidth exceeds ω_φ.

The rotating-wave approximation (RWA) is made for both the electric and magnetic field interactions, consistent with the small 1-photon detuning Δ together with a small 2-photon detuning of the EB^* process ($\omega_\varphi << \omega$). A magnetic interaction of the form $\hat{H}_{\text{int}}^{(m)} = -\mu_{eff}\bar{O}\cdot(\bar{L}\times\bar{B}/\hbar^2)$ is introduced in order to include torque in the dynamics (see Appendix B). In operator form this interaction Hamiltonian is:

$$\hat{H}_{\text{int}} = \hat{H}_{\text{int}}^{(e)} + \hat{H}_{\text{int}}^{(m)} = \hbar g(\hat{\sigma}^+\hat{a}^- + h.c.) + (\hbar f\hat{L}'_-\hat{O}'_+\hat{a}^+ + h.c.). \tag{2.5}$$

Primes on the orbital ($\hat{L}'_\pm \equiv \hat{L}_\pm/\hbar$) and rotational angular momentum operators ($\hat{O}'_\pm \equiv \hat{O}_\pm/\hbar$) indicate division by $\hbar$. The interaction strengths are $\hbar g \equiv -\mu_0^{(e)}\xi$ and $\hbar f \equiv -i\mu_{eff}\xi/c$, where $\mu_{eff} \equiv (2\omega_0/\omega_c)\mu_0^{(m)}$ is the effective magnetic moment; $\xi \equiv \sqrt{\hbar\omega/2\varepsilon_0 V}$ is the electric field per photon. The full Hamiltonian is $\hat{H} = \hat{H}_{mol} + \hat{H}_{field} + \hat{H}_{\text{int}}$, and the corresponding eigenvalue equation is $\hat{H}|D\rangle = E_D|D\rangle$ in the uncoupled basis, with

$$H = \begin{pmatrix} E_3 & 2\hbar f\sqrt{n} & 0 \\ 2\hbar f^*\sqrt{n} & E_2 & \hbar g\sqrt{n} \\ 0 & \hbar g^*\sqrt{n} & E_1 \end{pmatrix}. \tag{2.6}$$

The secular equation

$$\left(H - E_{Di}I\right)\left|D_i(n)\right\rangle = 0, \tag{2.7}$$

Optics EXPRESS

may be solved to determine the "doubly-dressed" eigenstates $|D_i(n)\rangle$ and their eigenenergies E_{Di}. For this purpose we set the secular determinant equal to zero.

$$\begin{vmatrix} E_3 - E_{Di} & 2\hbar f\sqrt{n} & 0 \\ 2\hbar f^*\sqrt{n} & E_2 - E_{Di} & \hbar g\sqrt{n} \\ 0 & \hbar g^*\sqrt{n} & E_1 - E_{Di} \end{vmatrix} = 0 \tag{2.8}$$

Equation (2.8) has the general form

$$y^3 + py^2 + qy + r = 0, \tag{2.9}$$

where $y = E_{Di}$, and the coefficients are

$$p \equiv -(E_1 + E_2 + E_3) \tag{2.10}$$

$$q \equiv (E_1E_2 + E_2E_3 + E_3E_1 - 4n\hbar^2|f|^2 - n\hbar^2g^2) \tag{2.11}$$

$$r \equiv (-E_1E_2E_3 + 4n\hbar^2|f|^2 E_1 + n\hbar^2g^2E_3). \tag{2.12}$$

With the additional replacement $y = x + p/3$, Eq. (2.9) reduces to

$$x^3 + ax + b = 0, \tag{2.13}$$

with new coefficients

$$\begin{aligned} a &= \frac{1}{3}(3q - p^2) \\ &= (E_1E_2 + E_2E_3 + E_3E_1 - 4n\hbar^2|f|^2 - n\hbar^2g^2) - \frac{1}{3}(E_1 + E_2 + E_3)^2 \end{aligned} \tag{2.14}$$

$$\begin{aligned} b &= \frac{1}{27}(2p^3 + 27r - 9pq) \\ &= \frac{2}{27}(E_1 + E_2 + E_3)^3 + (-E_1E_2E_3 + 4n\hbar^2|f|^2 E_1 + n\hbar^2g^2E_3) \\ &+ \frac{1}{3}(E_1 + E_2 + E_3)(E_1E_2 + E_2E_3 + E_3E_1 - 4n\hbar^2|f|^2 - n\hbar^2g^2) \end{aligned} \tag{2.15}$$

The solutions of Eq. (2.13) are given by

$$x_k = 2\sqrt{-\frac{a}{3}}\cos\left(\phi - k\frac{2\pi}{3}\right), \quad k = 0,1,2 \tag{2.16}$$

where the phase angle ϕ is defined by

$$\phi = \frac{1}{3}\cos^{-1}\left(\frac{3b}{2a}\sqrt{\frac{-3}{a}}\right). \tag{2.17}$$

Hence the analytic solutions for the doubly-dressed system are

$$E_{D1} = 2\sqrt{-\frac{a}{3}}\cos\left(\phi - \frac{4\pi}{3}\right) + \frac{1}{3}(E_1 + E_2 + E_3) \tag{2.18}$$

Optics EXPRESS

$$E_{D2} = 2\sqrt{-\frac{a}{3}}\cos\left(\phi - \frac{2\pi}{3}\right) + \frac{1}{3}(E_1 + E_2 + E_3) \tag{2.19}$$

$$E_{D3} = 2\sqrt{-\frac{a}{3}}\cos(\phi) + \frac{1}{3}(E_1 + E_2 + E_3) \tag{2.20}$$

where the subscripts have been chosen so that E_{D1} and E_{D2} reduce to the eigenenergies of a 2-level atom dressed by the electric field alone [16], and E_{D3} is the additional eigenenergy introduced when the magnetic field is considered.

Eigenstates $|D_i(n)\rangle$ of the system including both the electric and magnetic field couplings must satisfy the equation $(H - E_{Di}I)|D_i(n)\rangle = 0$. The states are expanded in terms of the basis states according to

$$|D_i(n)\rangle = a_i|1\rangle + b_i|2\rangle + c_i|3\rangle, \quad (\mathrm{i} = 1,2,3) \tag{2.21}$$

and the coefficients a_i, b_i, and c_i must satisfy the standard normalization condition

$$1 = |a_i|^2 + |b_i|^2 + |c_i|^2. \tag{2.22}$$

Because of the complexity of the roots, it is most convenient to display solutions of (2.7) in terms of the eigenenergies E_{Di} given in Eqs. (2.18-2.20). The eigenstates then acquire the form

$$|D_i(n)\rangle = \frac{1}{\Xi_i}\left[\left(\frac{(E_{Di} - E_2)}{\hbar g\sqrt{n}} - \frac{4\hbar|f|^2}{g(E_{Di} - E_3)}\right)|1\rangle + (1)|2\rangle + \left(\frac{2\hbar|f|^2}{(E_{Di} - E_3)}\right)|3\rangle\right], \tag{2.23}$$

where normalization is provided by the dimensionless factor

$$\Xi_i = \sqrt{\left(\frac{E_{Di} - E_2}{\hbar g\sqrt{n}} - \frac{4\hbar|f|^2}{g(E_{Di} - E_3)}\right)^2 + 1^2 + \left(\frac{2\hbar|f|^2}{(E_{Di} - E_3)}\right)^2}. \tag{2.24}$$

In the limit of negligible magnetic coupling ($\mathrm{f} \to 0$), the eigenstates in Eq. (2.22) reduce to the well-known quasi-eigenstates of an atom dressed by the electric field alone [16].

3. Results

The nonlinear magnetic dipole moment of interest here arises from charge motion that is induced by the two fields E and H^*. It can be thought of as motion initiated by the electric field that is subsequently deflected by the magnetic field of light. The magnetic moment is therefore expected to be proportional to the electric polarization and indeed the two leading contributions to the expectation value share this proportionality. Examination of the admixtures coupled by arrows in Fig. 2 reveals that the magnetization is one of two nonlinear dipoles that form according to standard selection rules among admixed components of the eigenstates. One is a nonlinear ED moment $p_z^{(2)}(0)$ that is oriented longitudinally with respect to the propagation axis. It lies perpendicular to the quantization axis, and couples the ground state admixtures $|21-1\rangle$ and $|100\rangle$, as indicated by the curved double-headed arrow in Fig. 2. The radiant magnetization is transverse to the propagation axis and couples $|210\rangle$

Optics EXPRESS

and $|21-1\rangle$. Its expectation value in terms of the slowly-varying amplitude of the density matrix $\tilde{\rho}$ [17] is

$$\begin{aligned}\langle \hat{m} \rangle &= Tr\left(\mu^{(m)}, \tilde{\rho}\right) \\ &= (\mu_{21}^{(m)}\tilde{\rho}_{12} + \mu_{31}^{(m)}\tilde{\rho}_{13} + \mu_{32}^{(m)}\tilde{\rho}_{23}) + c.c.\end{aligned} \tag{2.25}$$

Since $\mu_{21}^{(m)} = 0$, only two contributions to $\langle \hat{m} \rangle$ are non-zero. One is second order, and is observable as the *y*-projection of a 2-photon, magneto-electric moment that couples states 1 and 3. Such a projection can be implemented experimentally by passing the signal through a crossed polarizer. This contribution accounts for the portion of theoretical results in Fig. 3 at low input intensities (low photon number). The other is third order and accounts for saturation of the magnetization curves at high intensities. Multiple curves are shown in Fig. 3 to illustrate the dependence of nonlinear response on rotation frequency in the molecular model.

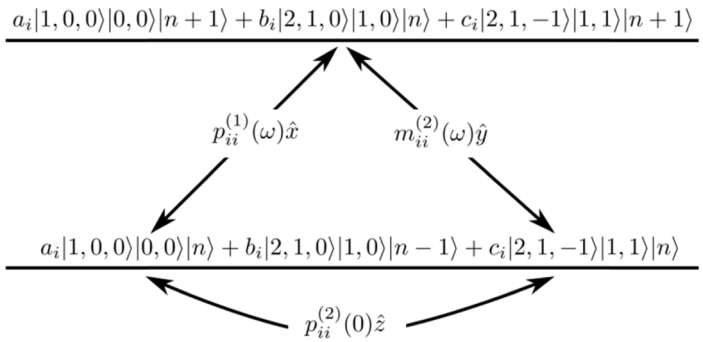

Fig. 2. Dressed state picture of three dipole moments formed by strong excitation of a nominally 2-level molecule during a 2-photon EB^* process. $p^{(1)}(\omega)\hat{x}$ is the linear *ED* polarization along the quantization axis. $p^{(2)}(0)\hat{z}$ and $m^{(2)}(\omega)\hat{y}$ are nonlinear rectification and magnetization moments oriented along $\hat{z}$ and $\hat{y}$ respectively.

The second-order term in the magnetic moment is the result of simultaneous ED and MD transitions which comprise an allowed, nearly resonant 2-photon transition between states 1 and 3 (see Appendix B). Since the two dipole transition moments that form the associated 2-photon coherence are orthogonal, they can be measured independently in experiments. The measured magnetic moment for example is the $\hat{y}$ projection of the second-order, magneto-electric coherence and radiates at the optical frequency.

$$\langle \hat{m}^{(2)} \rangle = [\mu_{13}^{me}\tilde{\rho}_{31}^{(2)}]_y + c.c. \tag{2.26}$$

The solution for the off-diagonal density matrix element is

$$\tilde{\rho}_{13}^{(2)} = \frac{\tilde{\rho}_{12}^{(1)}\tilde{V}_{23}^{(1)}}{\Delta_{13} + i\Gamma_{13}}, \tag{2.27}$$

where $\Delta_{13} \equiv (\omega_1 - \omega_3) - \omega$. The correspondence between density matrix elements and mixing coefficients in the dressed state picture is therefore $\tilde{\rho}_{12}^{(1)} \leftrightarrow a_i b_i^*$ and $\tilde{V}_{23}^{(1)}\mu_{31}^{(me)} / (\Delta_{13} + i\Gamma_{13}) \leftrightarrow \langle D_i | \mu_{21}^{(e)} \xi \mu_{eff}^{(m)} \hat{L}'_- \hat{O}'_+ \hat{\sigma}_+ | D_i \rangle$. Hence

Optics EXPRESS

$$\begin{aligned}\left\langle \hat{m}^{(2)} \right\rangle &= \left\{ a_i b_i^* \left\langle D_i \left| \mu_{12}^{(e)} \xi \mu_{eff}^{(m)} \hat{L}'_- \hat{O}'_+ \hat{\sigma}_+ \right| D_i \right\rangle + h.c. \right\}_y \\ &= a_i b_i^* \left\langle n \left| \langle 11 | \langle 21,-1 | c_i^* \mu_{eff}^{(m)} \hat{L}'_- \hat{O}'_+ b_i \left| 210 \right\rangle \right| 10 \right\rangle \left| n \right\rangle + h.c. \\ &= 2 a_i b_i^* b_i c_i^* \mu_{eff}^{(m)} \left\langle 11 \right| \left\langle 21,-1 \right| 21,-1 \left\rangle \right| 11 \right\rangle + c.c. \\ &= 2 c \mu_{12}^{(e)} (a_i b_i^* b_i c_i^* + c.c.)\end{aligned} \tag{2.28}$$

In Eq. (2.28) the effective magnetic moment has been replaced in the last step by $\mu_{eff}^{(m)} = c\mu_{12}^{(e)}$. This value is twice the upper bound on $\mu_{eff}^{(m)}$ derivable from Faraday's Law for a single component of angular momentum [7]. Because the initial state of the magnetic transition, namely $\left|210\right\rangle$, comprises two orbital angular momentum components with no net projection of L on the quantization axis, the maximum value for the quantum mechanical magnetic moment is twice the classical limit derived in [7]. Note that this upper bound represents the *upper limit* of magnetic enhancement calculated in Appendix B.

An additional contribution to $\left\langle \hat{m} \right\rangle$ arises from third order terms in the expectation value. In this case the measured moment is not proportional to a cross-polarized quadrature of a mixed moment, but to a magnetic dipole moment $\mu^{(m)}$ driven by a purely magnetic interaction on the transition between states 2 and 3.

$$\left\langle \hat{m}^{(3)} \right\rangle = \mu_{23}^{(m)} \rho_{32}^{(3)} + c.c. \tag{2.29}$$

The solution for the off-diagonal density matrix element in this case is

$$\tilde{\rho}_{23}^{(3)} = \frac{V_{21}^{(1)} \tilde{\rho}_{13}^{(2)}}{\Delta_{23} + i\Gamma_{23}}, \tag{2.30}$$

where $\Delta_{23} \equiv (\omega_2 - \omega_3) - \omega$. Only a single term contributes to (2.29) since $\mu_{21}^{(m)} = 0$ and $\mu_{31}^{(m)} = 0$. The coherence on the right side of Eq. (2.30) is second order (unlike that in Eq. (2.27)) and the magnetic moment forms in third order. Making use of the replacements $\tilde{\rho}_{13}^{(2)} \leftrightarrow a_i c_i^*$ and $\tilde{V}_{21}^{(1)} \mu_{32}^{(m)} / (\Delta_{23} + i\Gamma_{23}) \leftrightarrow \left\langle D_i \left| \mu_{21}^{(e)} \xi 2 \mu_{eff}^{(m)} \hat{\sigma}_+ \right| D_i \right\rangle$ one finds

$$\begin{aligned}\left\langle \hat{m}^{(3)} \right\rangle &= \left\{ a_i c_i^* \left\langle D_i \left| \mu_{21}^{(e)} \xi 2 \mu_{eff}^{(m)} \hat{\sigma}_+ \right| D_i \right\rangle + h.c. \right\}_y \\ &= 2 a_i c_i^* \left\langle n \left| \langle 10 | \langle 210 | b_i^* \mu_{eff}^{(m)} \hat{\sigma}_+ a_i \left| 100 \right\rangle \right| 00 \right\rangle \left| n \right\rangle + h.c. \\ &= 2 a_i^* b_i a_i c_i^* \mu_{eff}^{(m)} \left\langle 10 \right| \left\langle 210 \right| 210 \left\rangle \right| 10 \right\rangle + c.c. \\ &= 2 c \mu_{12}^{(e)} (a_i^* b_i a_i c_i^* + c.c.)\end{aligned} \tag{2.31}$$

In the last step of Eq. (2.31) the effective magnetic moment has been replaced by the upper bound $\mu_{eff}^{(m)} = c\mu_{12}^{(e)}$, as before. The total magnetic moment is given by the incoherent addition of Eqs. (2.28) and (2.31).

$$\left\langle \hat{m}(\omega) \right\rangle = 2 c \mu_{12}^{(e)} \left\{ \sum_{j=1}^{3} \left(a_j b_j^* a_j c_j^* + c.c. + a_j b_j^* b_j c_j^* + c.c. \right)^2 \right\}^{1/2}. \tag{2.32}$$

Optics EXPRESS

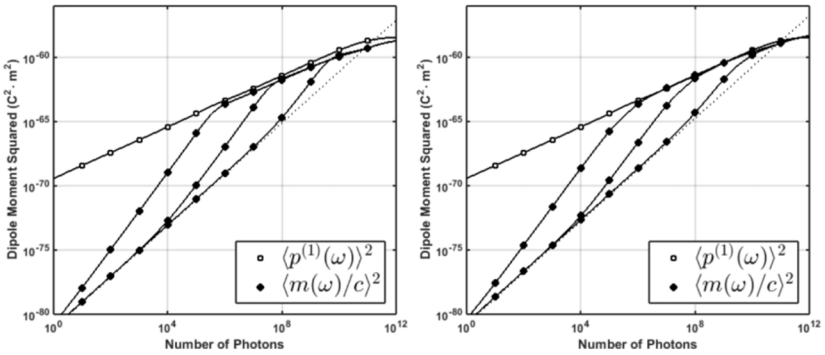

Fig. 3. Squared values of the total magnetic moment and the first order electric dipole moment versus the number of incident photons in the (a) 3-state model and (b) the 4-state model. In both figures separate curves are shown for $\langle \hat{m} \rangle^2$ with rotational frequencies (left to right) of $\omega_\varphi / \omega_0 = 10^{-7}, 10^{-5}, 10^{-3}$.

Results for the magnitude of the induced magnetic moment given by Eq. (2.32) are compared with that of the linear electric dipole moment $p^{(1)}(\omega)$ in the curves of Fig. 3(a). The electric dipole transition moment was arbitrarily chosen to be that of the principal resonance of hydrogen. Figure 3(a) shows the results for the analytic 3-state model of Section 2. Figure 3(b) presents results for the 4-state model, with basis state $|211\rangle$ included. A strong dependence of $\langle \hat{m}(\omega) \rangle$ on rotational frequency ω_φ is apparent in both plots. Results in Fig. 3(b) are numerically exact, and are very similar to those in Fig. 3(a), differing only by an increase in the predicted $\langle \hat{m}(\omega) \rangle$ values by a factor of $\sqrt{2}$ or roughly 30% due to the fourth basis state. The right side of the plots in Fig. 2 has been chosen to end at the ionization regime where even the linear polarization of the system saturates and numerical instabilities are encountered.

4. Conclusions

The general behavior of induced magnetic moments in this model may be described as follows. At low intensities in Figs. 3(a) and 3(b) the square of the nonlinear magnetic moment is quadratic with respect to input intensity. At higher input intensities the calculation of $\langle m \rangle^2$, which is proportional to magnetic scattering intensity, manifests a cubic dependence over a short range, and the curve for m saturates where it intersects that of p. In the saturation regime, the magnetization maintains a linear dependence on intensity, in strict proportion to the (linear) electric polarization. Both the ED and MD moments cease to increase when the ionization threshold is approached (on the far right of Fig. 3).

The present theoretical approach does not require uncommon or specialized ground state structure, but applies to simple molecules with symmetric ground states in which there is initially no angular momentum. From the results one may conclude that magnetic moments driven jointly by the electric and magnetic fields of light can grow to equal the electric dipole moment in molecular systems. The intensity I_{sat} at which saturation occurs depends on structural aspects of the medium that affect the 2-photon detuning, such as the libration frequency of the system. Based on Fig. 3, I_{sat} is proportional to rotation/libration frequency ω_φ. In molecular liquids the rotation frequency is $\omega_\varphi = \hbar / I$, so an inverse dependence of the induced magnetic moment on moment of inertia is expected. In solids there is no well-defined

Optics EXPRESS

moment of inertia at the molecular level. Nevertheless librational frequencies associated with localized optical centers are well-defined and may again be represented by ω_φ. Hence, the intensity requirement for saturated magnetization can be expected to drop in proportion to such characteristic frequencies in both liquids and solids. Other structural and chemical aspects of the medium, such as orientational damping and electron delocalization, doubtless affect the susceptibility of magneto-electric magnetization but will require further investigation.

Appendix A: ***Molecular rotational states***

The rotational states involved in the transfer of orbital to rotational angular momentum in magneto-electric interactions may be established by arguments based on parity of the levels and the magnetic interaction Hamiltonian derived in Appendix B. The following analysis applies to a *rigid rotor* model of the molecular system for which the magnetic interaction Hamiltonian is

$$\hat{H}_{\text{int}}^{(m)} = \hbar f \hat{L}'_{-} \hat{O}_{+}^{'} \hat{a}^{+} + h.c. \tag{A.1}$$

This interaction is rotationally invariant, so it commutes with the total angular momentum, which is $\hat{J} = \hat{L} + \hat{O}$ if spin is ignored (Hund's case b [18]). That is,

$$[\hat{H}_{\text{int}}^{(m)}, \hat{J}] = 0 \tag{A.2}$$

As a consequence of Eq. (A.2), total angular momentum is conserved in the interaction. Also the z-component of total angular momentum commutes with the Hamiltonian.

$$[\hat{H}_{\text{int}}^{(m)}, \hat{J}_z] = 0. \tag{A.3}$$

Forming a matrix element with the commutator in Eq. (A.3), one finds

$$\langle l'O'j'm'|[\hat{H}_{\text{int}}^{(m)}, \hat{J}_z]|lOjm\rangle = (m - m')\langle l'O'j'm'|\hat{H}_{\text{int}}^{(m)}|lOjm\rangle = 0. \tag{A.4}$$

Thus the matrix element $\langle l'O'j'm'|\hat{H}_{\text{int}}^{(m)}|lOjm\rangle$ vanishes unless $m = m'$. Since $\hat{J}_z = \hat{L}_z + \hat{O}_z$, and the eigenstates of $\hat{J}_z$ are also eigenstates of $\hat{L}_z$ and $\hat{O}_z$, the result $m = m'$ implies that initial and final projections of the total angular momentum must be equal.

$$m_l + m_o = m'_l + m'_o. \tag{A.5}$$

Next we note that possible values of total angular momentum for a given value of l must fall in the range $j = |l - O|, ..., l + O - 1, l + O$. Conversely, the possible values of O for a given value of j are $O = |j - l|, ..., j + l - 1, j + l$. Since $L = J = 1$ in the $|210\rangle$ excited state, which is the electronic state from which the magnetic transition is initiated, the only allowed values of O are $O = 0, 1, 2$. The parity of this state is determined by the parity of the rotational wavefunction [15]. Because $m_l = 0$ (denoted $\Lambda = 0$ in [15]) the parity in question is positive or negative according as O is even or odd. However the parity of the excited state must be negative in order to satisfy the electric dipole selection rule for an electric dipole (ED) transition from the ${}^1\Sigma_g^+$ ground state, which has positive parity. The rule for an ED transition is that the parity must change and m must not. The ground state rotational state is $|Om_o\rangle = |00\rangle$ by assumption, but in the excited state the rotational quantum number O must have one of the values $O = 0, 1, 2$ and be odd. Hence $O = 1$ in the electronic excited

Optics EXPRESS

state of our model and the complete rotational wavefunction in the upper state is therefore $|Om_o\rangle = |10\rangle$.

Next, note that for a magnetic dipole (MD) transition the parity of the initial and final states must be the same. This imposes the requirement that final and initial rotational angular momenta be the same, or $O' = O$. Now, to find the projection of rotational angular momentum on the quantization axis in the final state, note that the operator $\hat{L}'_-$ in $\hat{H}^{(m)}_{\text{int}}$ lowers the projection of orbital angular momentum without changing l. That is, $m'_l = -1$. Since the sum of upper state projections of angular momentum on the quantization axis yield $m_l + m_o = 0$, Eq. (A.5) requires that $m'_l + m'_o = 0$, or $m'_o = 1$. Thus the final orbital state is $|l', m'_l\rangle = |1,-1\rangle$ and the final rotational state is $|O', m'_o\rangle = |1,1\rangle$. These angular momentum states are exactly those expected from the ladder operators in the magnetic Hamiltonian, namely $\hat{L}'_- \hat{O}'_+ |210\rangle|10\rangle = 2|21-1\rangle|11\rangle$.

Appendix B: ***Magnetic interaction Hamiltonian***

Eigenstates of light carry an amount of intrinsic angular momentum equal to $\hbar$ per photon. Consequently in spinless atoms, where any induced magnetic moment $\bar{\mu} = (e/2m)\bar{L}$ depends on orbital angular momentum resulting from optical interactions, the magnetic response is invariably small, yielding moments on the order of $\mu_0^{(m)} \equiv (e/2m_e)\hbar$. In molecules however, orbital (internal) and rotational (external) angular momenta are coupled in a fashion reminiscent of the Einstein-de Haas effect [10], and this provides a mechanism for the enhancement of magnetic moments ($\mu_{eff} >> \mu_0^{(m)}$) as shown here.

To derive the full interaction Hamiltonian of Eq. (2.5), we consider it to be the sum of electric dipole (ED) and magnetic dipole (MD) interactions, with the effect of magnetic torque included in the magnetic transition in the excited state. Because the model has no ground state sub-levels, the interaction can only be initiated by an ED interaction from the true ground state. Then the kinematic effect of magnetic torque is to rotate the axis of orbital motion during the MD transition so as to leave the molecule in a pure rotational state. As a result, it is convenient to derive the torque interaction by starting from the rotational energy of the final state and connect it to the electronically excited state using components of the total angular momentum that can transfer momentum between internal and external coordinates.

The kinetic energy of molecular rotation is given by

$$H = \tfrac{1}{2} I\omega^2 = \tfrac{1}{2}\bar{\omega}\cdot\bar{O}, \tag{B.1}$$

where ω is the angular frequency about an axis perpendicular to the internuclear axis. I is the moment of inertia, and $\bar{O} = I\bar{\omega}$ is the angular momentum vector of the rigid rotor. If the rotational angular momentum $\bar{O}$ is due to torque $\bar{T}$ exerted by a magnetic field on internal angular momentum $\bar{L}$, it accumulates with time classically according to

$$\bar{O} = \int_0^{\Delta t} \left(\frac{d\bar{O}}{dt}\right) dt. \tag{B.2}$$

Also, if total angular momentum $\bar{J} = \bar{L} + \bar{O}$ is conserved, its time derivative is zero. Thus

$$d\bar{J}/dt = d(\bar{L} + \bar{O})/dt = 0, \tag{B.3}$$

and

Optics EXPRESS

$$\bar{O} = -\int_0^{\Delta t} \left(\frac{d\bar{L}}{dt} \right) dt. \tag{B.4}$$

The equation of motion for rotations is $\bar{T} = d\bar{L}/dt$ in a fixed reference frame. Magnetic torque is given by $\bar{T} = \bar{m} \times \bar{B}$, where $\bar{m}$ is the magnetic moment due to circulation of charge at the optical frequency. (Although there are no definite orbits in quantum mechanics, there is still circulation of the electron about the internuclear axis when $L \neq 0$.) The expression for $\bar{O}$ becomes

$$\bar{O} = -\int_0^{\Delta t} (\bar{m} \times \bar{B}) dt. \tag{B.5}$$

For molecules, constants of the motion and the moments determined by them are referenced to the molecular center-of-mass (COM). We may therefore specify electron position as $\bar{R} = \bar{r} + \bar{h}$ in cylindrical coordinates (r, φ, h) that are centered on an origin halfway between the nuclei of our diatomic, homonuclear rigid rotor. Prior to the application of magnetic torque, charge circulation responsible for $\bar{L}$ in the excited state is then purely azimuthal, as depicted in Fig. 4 and the axis of the molecule is stationary. The orbital momentum $\bar{L} = \bar{R} \times m_e (d\bar{R}/dt)$ contains four terms, three of which are then zero. m_e is the mass of the electron. The terms $\bar{r} \times m_e (d\bar{h}/dt)$ and $\bar{h} \times m_e (d\bar{h}/dt)$ are both zero because the axial component of $\bar{R}$ is time-invariant in a stationary molecule. Also $\bar{h} \times m_e (d\bar{r}/dt)$ does not contribute to the classical angular momentum since the product is directed radially along $\bar{r}$ and rotates at frequency ω_0, meaning it is not a constant of the motion in a diatomic molecule [15]. Hence,

$$\bar{L} = m_e \bar{r} \times \frac{d\bar{r}}{dt}, \tag{B.6}$$

and its magnitude is

$$L = m_e r^2 \omega_0, \tag{B.7}$$

since $\omega_0 \equiv |d\hat{r}/dt|$ is the classical resonant frequency of the molecule.

Next, the effect of the optical magnetic field is considered, in order to estimate the maximum enhancement of magnetic response that could result from molecular torque dynamics. The axis of initial orbital angular momentum is rotated by magnetic torque so that the angular momentum of the electron is transferred to an orientation perpendicular to the molecular axis. To conserve total angular momentum and energy, the molecule must undergo end-over-end rotations following the torque interaction, in an orbit about the center-of-mass coordinate that has a much larger radius than the initial one.

Optics EXPRESS

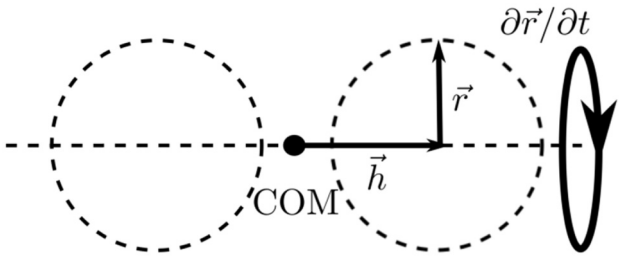

Fig. 4. Orbital angular momentum L of an electron about the internuclear axis of a diatomic molecule, visualized in cylindrical coordinates referenced to the center of mass (COM) and fixed in the molecule. No magnetic torque has been exerted on the system. Angular momentum is determined by coordinate r of the electron.

When the magnetic field exerts torque on the orbital angular momentum of the molecule, charge motion around the molecular axis ceases to be a constant of the motion. Motion is rotated into a plane orthogonal to the initial one, as shown in Fig. 5. Referring to the diagram, the rotational angular momentum can be expressed as $\bar{O} = \bar{R} \times m_e (d\bar{R}/dt)$, reducing to $\bar{O} \cong m_e h\hat{h} \times h(d\hat{h}/dt)$ for a rigid rotor ($dh/dt = 0$) in the limit $h >> r$. Energy is conserved while orbital kinetic energy is converted to motion in the plane of Fig. 5 via torque. So initial and final electron velocities are the same ($d\bar{r}/dt = d\bar{h}/dt$), although their orbital radii r and h are different. The nuclei are also assumed to follow the electron motion adiabatically. Consistent with this and Fig. 1, the interaction therefore concludes with the molecule executing rotations (librations) at the rotational frequency $\omega_\varphi \equiv d\hat{h}/dt$. Energy conservation requires that $r\omega_0 = h\omega_\varphi$ and the final rotational angular momentum of the system is approximately given by

$$\bar{O} \cong m_e h^2 \omega_\varphi \hat{r}_0 = m_e hr\omega_0 \hat{r}_0, \tag{B.8}$$

which has a magnitude of

$$O = m_e hr\omega_0. \tag{B.9}$$

In Eq. (B.8) carets denote unit vectors. So $\hat{r}_0 = \hat{L} \times \hat{B}$ is a unit vector perpendicular to the internuclear axis that determines the direction of $\bar{O}$.

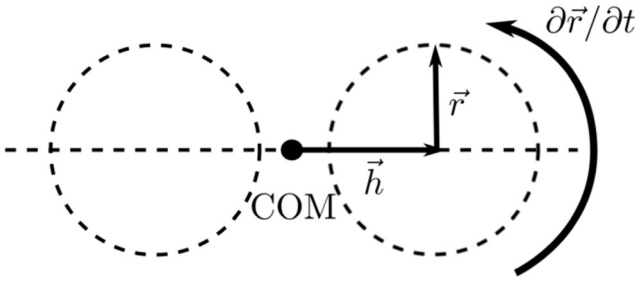

Fig. 5. After the application of magnetic torque, electron motion is in a plane orthogonal to that in Fig. 4. It consists of rotation about an axis perpendicular to the internuclear axis, normal to the plane of the drawing. Angular momentum is determined chiefly by coordinate h of the electron since we assume $h >> r$.

Optics EXPRESS

The distance h is one half the internuclear separation, whereas r is much smaller; it is an average radius of the excited state orbital with respect to the molecular axis $(h >> r)$. The relative magnitudes of $\bar{O}$ and $\bar{L}$ for the same electron velocity are therefore related by an enhancement factor η obtained by combining Eqs. (B.7) and (B.9).

$$\eta \equiv O / L \cong h / r. \tag{B.10}$$

An immediate consequence of this result is that following a full rotation of the axis through ninety degrees, the magnetic moment in Eq. (B.5) is enhanced.

$$\bar{m} = \eta \left(\frac{e\bar{L}}{2m_e} \right) \tag{B.11}$$

Thus the rotational angular momentum is given by the integral

$$\bar{O} = -\int_0^{\Delta t} \left(\frac{e\eta}{2m_e} \right) (\bar{L} \times \bar{B}) dt. \tag{B.12}$$

In a classical setting the initial angular momentum is time dependent, since it is proportional to electron velocity which in turn is driven by the electric field $\bar{E} = \frac{1}{2}(\bar{E}_0 e^{i\omega t} + \bar{E}_0^* e^{-i\omega t})$. We assume the field is real ($\bar{E}_0 = \bar{E}_0^*$) and that $\bar{L}$ and $\bar{B}$ have similar forms. Then, the slowly-varying amplitude of the rotational angular momentum in Eq. (B.12) yields

$$\bar{O} = -\left(\frac{e\eta}{2m_e} \right) \left(\frac{2\bar{L}_0 \times \bar{B}_0^*}{4} \right) \Delta t. \tag{B.13}$$

By substituting this result for $\bar{O}$ into the kinetic energy we obtain

$$H = -\frac{1}{2I} \frac{e\eta}{2m_e} \bar{O} \cdot \left(\frac{\bar{L}_0 \times \bar{B}_0^*}{2} \right) \Delta t = -\frac{1}{2I} \bar{\mu}_{\hat{O}} \cdot \left(\frac{\bar{L}_0 \times \bar{B}_0^*}{2} \right) \Delta t, \tag{B.14}$$

where the rotational magnetic moment is defined to be $\bar{\mu}_{\hat{O}} \equiv \eta \left(\frac{e\hbar}{2m_e} \right) \bar{O}'$ and $\bar{O}' \equiv \bar{O} / \hbar$.

The momentum transfer time interval Δt may be estimated from Eq. (B.14) by setting the time-integrated torque equal to the orbital angular momentum available for transfer, which is $\hbar$ (for an $L = 1$ excited state). That is,

$$\Delta \bar{L} = \left(\frac{e}{2m_e} \right) \left(\frac{\bar{L}_0 \times \bar{B}_0^*}{2} \right) \Delta t = \hbar \hat{O}. \tag{B.15}$$

Setting $L_0 = \hbar$ also, and solving for Δt, one finds

$$\Delta t = \frac{4m_e}{eB_0^*} = \frac{4}{\omega_c}, \tag{B.16}$$

where $\omega_c \equiv eB_0 / m_e$. Using these results for the inter-conversion of components of the total angular momentum, it is possible to connect the rotation of a molecule to its excited state orbital motion via a torque-mediated transition embodied in the interaction Hamiltonian

Optics EXPRESS

$$H_{\text{int}} = -\left(\frac{2\omega_\varphi}{\omega_c}\right)\bar{\mu}_{\hat{O}} \cdot (L \times \bar{B}) = -\mu_{eff}\bar{O}' \cdot (L \times \bar{B}). \tag{B.17}$$

The effective magnetic moment $\mu_{eff} \equiv \eta(2\omega_\varphi / \omega_c)\mu_0^{(m)}$ in Eq. (B.17) incorporates the relation between rotation frequency and moment of inertia ($\omega_\varphi \equiv \hbar / I$), as well as a reference moment associated with the minimum possible quantized value of angular momentum, namely $\mu_0^{(m)} \equiv (e\hbar / 2m_e)$. As in the body of this paper, primes on angular momentum operators indicate division by $\hbar$. On the basis of Eq. (B.8) the enhancement factor can also be expressed in terms of measurable, characteristic frequencies of the system as $\eta = h / r = \omega_0 / \omega_\varphi$. As a consequence, the effective magnetic moment takes on the particularly simple form of

$$\mu_{eff} = \left(\frac{2\omega_0}{\omega_c}\right)\mu_0^{(m)}. \tag{B.18}$$

Because the optical frequency is much larger than the cyclotron frequency at low to moderate intensities, the estimated ratio of the effective to the reference magnetic moment exceeds the inverse fine structure constant ($\mu_{eff} / \mu_0^{(m)} >> \alpha^{-1}$), placing ED and MD moments on a par. Note that Eq. (B.18) appears to suggest that progressively smaller cyclotron frequencies, or weaker magnetic field amplitudes B_0, yield arbitrarily large magnetic moments. However the torque interaction must take place in a time less than the excited state decay time τ_{rad}. Hence, based on Eq. (B.16), B_0 is restricted to the range $B_0 \geq 4m_e / e\tau_{rad}$.

Next, correspondence is applied to write the Hamiltonian (B.17) in operator form. $\bar{B}$ is taken to lie along $\hat{y}$, $\bar{E}$ along the quantization axis $\hat{x}$, parallel to the molecular axis.

$$\bar{L}' \times \hat{y} = L_x'\hat{z} - L_z'\hat{x} \tag{B.19}$$

$$\bar{O}' \cdot (\bar{L}' \times B\hat{y}) = \bar{O}' \cdot (L_x'\hat{z} - L_z'\hat{x})B = (O_z'L_x' - O_x'L_z')B \tag{B.20}$$

Since the component of angular momentum along the quantization axis L_x' contributes only diagonal matrix elements, it may be omitted from the interaction Hamiltonian. Hence

$$\hat{H}_{\text{int}} = -\mu_{eff}\hat{O}_x'\hat{L}_z'\hat{B}, \tag{B.21}$$

where carets indicate operators. Note that $\hat{L}_z'$ is a transverse component of $\hat{L}'$ while $\hat{O}_x'$ is a transverse component of $\hat{O}'$, in view of the orthogonality of $\bar{L}$ and $\bar{O}$. Consequently

$$\hat{L}_z' = \tfrac{1}{2i}(\hat{L}_+' - \hat{L}_-') \tag{B.22}$$

$$\hat{O}_x' = \tfrac{1}{2i}(\hat{O}_+' - \hat{O}_-') \tag{B.23}$$

Taken together with the operator form of the magnetic field, these expressions yield

$$\hat{H}_{\text{int}} = -\mu_{eff}\frac{1}{2i}(\hat{O}_+' - \hat{O}_-')\frac{1}{2i}(\hat{L}_+' - \hat{L}_-')i(\hat{a}^+ - \hat{a}^-)\xi / c, \tag{B.24}$$

where $\xi \equiv \sqrt{\hbar\omega / 2\varepsilon_0 V}$ is the electric field per photon. The secular form of Eq. (B.24) is

$$\hat{H}_{\text{int}} = -i\mu_{eff}(\hat{O}_+'\hat{L}_-'\hat{a}^+ - \hat{O}_-'\hat{L}_+'\hat{a}^-)\xi / c \tag{B.25}$$

Optics EXPRESS

or

$$\hat{H}_{\text{int}} = \hbar f \hat{L}_{-} \hat{O}'_{+} \hat{a}^{+} + h.c., \tag{B.26}$$

when the magnetic interaction Hamiltonian is expressed in terms of an enhanced coupling energy $\hbar f \equiv -i\mu_{eff}\xi / c$.

Funding

Air Force Office of Scientific Research (AFOSR) (FA9550_12_1_0119 and FA9550_14_1_0040).

Acknowledgments

This research was supported by the MURI Center for Dynamic Magneto-optics. E.F.C.D. gratefully acknowledges an NSF graduate research fellowship.